Computers, Materials & Continua
DOI: 10.32604/cmc.2023.018637
Article

Throughput Analysis of HARQ Scheme Based on Full-Duplex Two-Way AF SWIPT Relay

Xiaoye Shi[1,*], Fei Ding[1,2], Haiting Zhu[1], Zhaowei Zhang[1] and Lei Zhang[1]

[1]School of Internet of Things (Nanjing University of Posts and Telecommunications), Nanjing, 210003, China
[2]Department of Electronic and Electrical Engineering (University College London), London, WC1E6BT, UK
*Corresponding Author: Xiaoye Shi. Email: shixy187@njupt.edu.cn
Received: 15 March 2021; Accepted: 18 April 2021

Abstract: The simultaneous wireless information and power transfer (SWIPT) relay system is one of the emerging technologies. Xiaomi Corporation and Motorola Inc. recently launched indoor wireless power transfer equipment is one of the most promising applications. To tap the potential of the system, hybrid automatic repeat request (HARQ) is introduced into the SWIPT relay system. Firstly, the time slot structure of HARQ scheme based on full duplex two-way amplify and forward (AF) SWIPT relay is given, and its retransmission status is analyzed. Secondly, the equivalent signal-to-noise ratio and outage probability of various states are calculated by approximate simplification. Thirdly, the energy harvesting power in each state is calculated. Finally, the energy harvested-throughput sum function is constructed to characterize the performance of energy harvesting and data transmission. Simulation results show that the proposed HARQ scheme has better energy harvested-throughput sum function than the traditional HARQ scheme. When $P_2 = 22$ dB, the maximum sum function is 54.86% (the proposed HARQ scheme) and 52.307% (the traditional HARQ scheme), respectively.

Keywords: SWIPT; relay; HARQ; throughput; full-duplex

1 Introduction

With the realization of wireless power transfer technology of cellular network [1–3] and sensor networks [4,5], new researches upsurge appear. Because it is not limited to the battery capacity, the simultaneous wireless information and power transfer (SWITP) technology makes the battery's super long endurance becomes a reality [6]. Xiaomi Corporation and Motorola Inc. recently launched indoor wireless power transfer equipment is one of the most promising applications. By amplifying and forwarding the received signal, the relay can not only help the information transmission, but also promote the wireless power transfer [7,8]. Two-way full-duplex relay can further improve the information transmission efficiency of the SWIPT relay system, with providing more flexible transmission strategy [9,10].

The hybrid automatic repeat request (HARQ) technology improve the reliability of data transmission through error detection and data retransmission [11]. Furthermore, HARQ improve the effectiveness of the system by the maximum ratio combining of the data received [12,13]. In [14], the HARQ technology was applied in two-way communication. The research show that the transmission capacity obtained by full duplex transmission and packet retransmission through HARQ protocol exceeds the loss caused by bidirectional use and HARQ. In order to improve the throughput of the system, full duplex relay was used in [15], and a reverse link assisted network coding HARQ with indirect information was used at the relay port. Reference [16] studied the performance of full duplex cooperative networks under HARQ from two aspects of data link layer packet error rate (per) and master-slave throughput. The cooperative relay scheme without initialization phase is proposed to realize HARQ retransmission assisted by complex relay [17].

How to combine HARQ technology with SWIPT technology to improve the efficiency of data and energy transmission is a fascinating novel subject. Reference [18] propose the optimal strategy aiming at the minimum expected retransmission times and accumulate mutual information. Unfortunately, for SWIPT systems, accumulate mutual information are not comprehensive. This paper mainly studies the application of energy carrying relay and HARQ in full duplex two-way amplify and forward (AF) relay system. According to the characteristics of full-duplex two-way AF relay and energy carrying relay, a HARQ scheme based on full-duplex two-way AF relay is proposed, and its performance is analyzed. Based on this, the following work is done: a) The slot structure of HARQ scheme based on full duplex bidirectional AF energy carrying relay is given, and its retransmission status is analyzed. b) The equivalent signal-to-noise ratio and outage probability of various states are calculated by approximate simplification. c) The power of energy harvesting in each state is calculated. d) The sum function of throughput-energy harvesting is constructed, and the performance of data transmission and energy harvesting is characterized.

2 System Model of the Full-Duplex Two-Way SWIPT Relay System

Fig. 1 is the system diagram of full-duplex two-way SWIPT relay system, which is composed of two terminals T_1, T_2 and relay node R. The system consists of four communication links including direct link between T_1 and T_2 and two swift links, in which energy is transmitted from relay node to two terminals. In this system, the relay node R adopts the AF mode, and also takes into account the role of energy transmission. Terminal nodes T_1 and T_2 adopt full duplex mode, that is, nodes can also send data at the same time when receiving data, so as to obtain transmission rate more efficiently, but also cause self-interference problem. The access mode of the system is time division multiple access (TDMA).

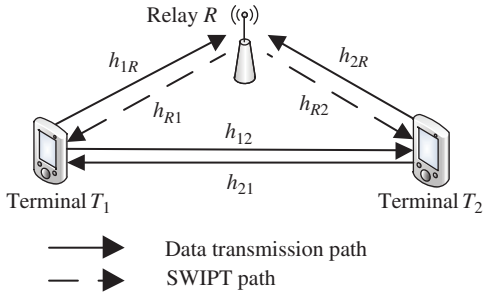

Figure 1: System model of the full-duplex two-way SWIPT relay system

h_{ab} ($a \in \{1,\ R,\ 2\}$, $b \in \{1,\ R,\ 2\}$) is used to represent the channel gain of each channel, which follows the complex Gaussian distribution with mean value of 0 and variance of σ_{ab}^2 ($a \in \{1,\ R,\ 2\}$, $b \in \{1,\ R,\ 2\}$) (where h_{11} and h_{22} are the channel gain of self-interference channel); n_{ab}^c ($a \in \{1,\ R,\ 2\}$, $b \in \{1,\ R,\ 2\}$) is used to represent the circuit noise caused by energy harvesting, which is subject to complex Gaussian distribution with mean value of 0 and variance of N_{ab}^c ($a \in \{1,\ R,\ 2\}$, $b \in \{1,\ R,\ 2\}$); n_{ab}^e ($a \in \{1,\ R,\ 2\}$, $b \in \{1,\ R,\ 2\}$) is used to represent the equivalent noise caused by signal demodulation, which obeys the complex Gaussian distribution with mean value of 0 and variance of N_{ab}^e ($a \in \{1,\ R,\ 2\}$, $b \in \{1,\ R,\ 2\}$). The total transmission power of the system is P_T, and the power allocated to two terminals T_1, T_2 and relay R is P_1, P_2 and P_R, *i.e.*, $P_1 + P_2 + P_R = P_T$. Assuming that the uplink channel and downlink channel are symmetric channels, then $h_{ab} = h_{ba}$ ($\forall a \in \{1,\ R,\ 2\}$, $b \in \{1,\ R,\ 2\}$).

3 System Slot Structure of the Full-Duplex Two-Way SWIPT Relay System

As shown in Tab. 1, the system is divided into two time slots. In the first time slot, data are transmitted and received by two terminals T_1 and T_2 at the same time, and the relay node receives the mixed signal of the two terminals. Terminal T_1 and T_2 detect the received signal cyclic redundancy check (CRC) to determine whether the system needs retransmission. The second time slot is the SWIPT time slot, and the relay node sends the retransmission data and energy simultaneously. The second time slot is divided into four states: when two terminals in one time slot receive data successfully, the relay node only transmits energy; when both terminals in the first slot fail to receive data successfully, the relay node mainly transmits data, supplemented by energy transmission; when only one terminal in the first slot receives data successfully, the terminal receiving data successfully mainly transmits energy and another terminal is mainly for data transmission.

Table 1: System time slot structure

	First time slot	Second time slot (four states)			
		T_1 succeeded, T_2 succeeded	T_1 succeeded, T_2 failed	T_1 failed, T_2 succeeded	T_1 failed, T_2 failed
Terminal T_1	Send data x_1 and receive data from T_2.	WPT status: only receiving energy	WPT status: only receiving energy	SWIPT status: simultaneously receiving data and energy	SWIPT status: simultaneously receiving data and energy
Terminal T_2	Send data x_2 and receive data from T_1.	WPT status: only receiving energy	SWIPT status: simultaneously receiving data and energy	WPT status: only receiving energy	SWIPT status: simultaneously receiving data and energy
Relay R	Receive the mixed data from T_1 and T_2	Forward amplified mixed data and energy to T_1 and T_2			

with x_1 and x_2 are the data to be transmitted by terminals T_1 and T_2 respectively.

In the first time slot, two terminals T_1 and T_2 transmit and receive data at the same time. The relay node receives the mixed signal of the two terminals, so the received signals of the three nodes are as follows:

$$y_{12} = \sqrt{P_1} * (h_{12} * x_1) + \sqrt{P_2} * h_{22} * x_2 + n_{12}^e, \tag{1}$$

$$y_{21} = \sqrt{P_2} * (h_{21} * x_2) + \sqrt{P_1} * h_{11} * x_1 + n_{21}^e, \tag{2}$$

$$y_R = \sqrt{P_1} * (h_{1R} * x_1) + \sqrt{P_2} * (h_{2R} * x_2) + n_R, \tag{3}$$

where n_R represents the noise signal received by the first time slot relay node, which obeys the complex Gaussian distribution with mean value of 0 and variance of N_R. $\sqrt{P_1} * (h_{12} * x_1)$ and $\sqrt{P_2} * (h_{21} * x_2)$ are the effective signals received by two terminals T_1 and T_2 respectively. $\sqrt{P_2} * h_{22} * x_2$ and $\sqrt{P_2} * (h_{11} * x_2)$ are self-interference signals. Therefore, the received signal-to-noise ratio (SNR) of two terminals T_1 and T_2 in the first time slot is $SNR_{21} = \dfrac{P_2 |h_{21}|^2}{P_1 |h_{11}|^2 + N_{21}^e}$ and $SNR_{12} = \dfrac{P_1 |h_{12}|^2}{P_2 |h_{22}|^2 + N_{12}^e}$ respectively.

The outage probability of T_1 and T_2 signals in the first slot is as follows:

$$\mathrm{P}_{out}^{12} = \Pr\left\{SNR_{12} < 2^{2R} - 1\right\} = 1 - \exp\left(-\frac{1}{\sigma_{12}^2} \frac{2^{2R} - 1}{\theta_{1,1}}\right), \tag{4}$$

$$\mathrm{P}_{out}^{21} = \Pr\left\{SNR_{21} < 2^{2R} - 1\right\} = 1 - \exp\left(-\frac{1}{\sigma_{21}^2} \frac{2^{2R} - 1}{\theta_{2,1}}\right), \tag{5}$$

where $\theta_{1,1} = \dfrac{P_2}{P_1 \sigma_{11}^2 + N_{21}^e}$, $\theta_{2,1} = \dfrac{P_1}{P_2 \sigma_{22}^2 + N_{12}^e}$.

In the second time slot, the relay node sends retransmission data and energy at the same time. At this moment, the received signals of the two terminals T_1 and T_2 can be expressed as follows:

$$y_{R1} = G * (h_{R1} * y_R) + n_{R1}^e, \tag{6}$$

$$y_{R2} = G * (h_{R2} * y_R) + n_{R2}^e, \tag{7}$$

where the amplification factor is $G = \sqrt{\dfrac{P_R}{P_1 |h_{1R}|^2 + P_2 |h_{2R}|^2 + n_R}}$.

If the two terminals are in the state of SWIPT in the second slot, the received information data are as follows:

$$y_{R1}^c = \sqrt{\tau} \left(G h_{R1} h_{2R} \sqrt{P_2} x_2 + G h_{R1} n_R + n_{R1}^e\right) + n_{R1}^c, \tag{8}$$

$$y_{R2}^c = \sqrt{\tau} \left(G h_{R2} h_{1R} \sqrt{P_1} x_1 + G h_{R2} n_R + n_{R2}^e\right) + n_{R2}^c, \tag{9}$$

with τ is the proportion of energy allocated to information reception, and the rest $1 - \tau$ is used for energy harvesting.

At this time, the received signal-to-noise ratio of terminal T_1 is:

$$\begin{aligned} SNR_{R1}^{c} &= \frac{\tau P_R P_2 \left|h_{R1}\right|^2 \left|h_{2R}\right|^2}{\tau P_R \left|h_{R1}\right|^2 N_{\mathrm{R}} + \left(\tau N_{R2}^{e} + N_{R2}^{c}\right)\left(P_1 |h_{1R}|^2 + P_2 |h_{2R}|^2 + N_{\mathrm{R}}\right)} \\ &= \frac{\theta_{1,5}\left|h_{R1}\right|^2 \left|h_{2R}\right|^2}{\theta_{1,2}\left|h_{R1}\right|^2 + \theta_{1,3}|h_{2R}|^2 + \theta_{1,4}} \\ &= \frac{\frac{\theta_{1,2}\theta_{1,3}}{\theta_{1,4}^{2}}\left|h_{R1}\right|^2 \left|h_{2R}\right|^2}{\frac{\theta_{1,2}}{\theta_{1,4}}\left|h_{R1}\right|^2 + \frac{\theta_{1,3}}{\theta_{1,4}}|h_{2R}|^2 + 1} \frac{\theta_{1,5}\theta_{1,4}}{\theta_{1,2}\theta_{1,3}} \end{aligned}, \tag{10}$$

where $\theta_{1,2} = \left(\tau P_R N_{\mathrm{R}} + \left(\tau N_{\mathrm{R2}}^{e} + N_{\mathrm{R2}}^{c}\right) P_1\right), \theta_{1,3} = P_2\left(\tau N_{\mathrm{R2}}^{e} + N_{\mathrm{R2}}^{c}\right), \theta_{1,4} = N_{\mathrm{R}}\left(\tau N_{\mathrm{R2}}^{e} + N_{\mathrm{R2}}^{c}\right), \theta_{1,5} = \tau P_R P_2$.

Similarly, the receiving signal-to-noise ratio (SNR) of terminal T_2 is as follows:

$$SNR_{R2}^{c} = \frac{\frac{\theta_{2,2}\theta_{2,3}}{\theta_{2,4}^{2}}\left|h_{R2}\right|^2 \left|h_{1R}\right|^2}{\frac{\theta_{2,2}}{\theta_{2,4}}\left|h_{R2}\right|^2 + \frac{\theta_{2,3}}{\theta_{2,4}}|h_{1R}|^2 + 1} \frac{\theta_{2,5}\theta_{2,4}}{\theta_{2,2}\theta_{2,3}}, \tag{11}$$

where $\theta_{2,2} = \left(\tau P_R N_{\mathrm{R}} + \left(\tau N_{\mathrm{R1}}^{e} + N_{\mathrm{R1}}^{c}\right) P_2\right), \theta_{2,3} = P_1\left(\tau N_{\mathrm{R1}}^{e} + N_{\mathrm{R1}}^{c}\right), \theta_{2,4} = N_{\mathrm{R}}\left(\tau N_{\mathrm{R1}}^{e} + N_{\mathrm{R1}}^{c}\right), \theta_{2,5} = \tau P_R P_1$.

4 System Throughput and Sum Function of the Full-Duplex Two-Way SWIPT Relay System

In order to briefly describe the receiving process, the following scenario of T_2 transmission and T_1 reception is taken as an example:

When the CRC detection of the first slot is successful, the power divider allocates all the energy to the energy harvesting, that is $\tau = 0$, the terminal is in WPT state at the moment. The power of energy harvesting is as follows:

$$E_1^{P} = \eta \sigma_{R1}^{2} P_R, \tag{12}$$

with η is the conversion efficiency of energy harvesting.

If the CRC detection of the first time slot fails, the terminal is in the SWIPT state. T_1 combines the signals about x_2 received by the two time slots with the maximum ratio, and the combined equivalent signal-to-noise ratio is the sum of twice received SNRs:

$$\begin{aligned} & SNR_{\mathrm{ARQ},1} \\ &= SNR_{21} + SNR_{R1}^{c} \\ &= |h_{21}|^2 \theta_{1,1} + \frac{\frac{\theta_{1,2}\theta_{1,3}}{\theta_{1,4}^{2}}\left|h_{R1}\right|^2 \left|h_{2R}\right|^2}{\frac{\theta_{1,2}}{\theta_{1,4}}\left|h_{R1}\right|^2 + \frac{\theta_{1,3}}{\theta_{1,4}}|h_{2R}|^2 + 1} \frac{\theta_{1,5}\theta_{1,4}}{\theta_{1,2}\theta_{1,3}} \\ &= \left(\frac{|h_{21}|^2 \theta_{1,1}\theta_{1,2}\theta_{1,3}}{\theta_{1,4}\theta_{1,5}} + \frac{\frac{\theta_{1,2}\theta_{1,3}}{\theta_{1,4}^{2}}\left|h_{R1}\right|^2 \left|h_{2R}\right|^2}{\frac{\theta_{1,2}}{\theta_{1,4}}\left|h_{R1}\right|^2 + \frac{\theta_{1,3}}{\theta_{1,4}}|h_{2R}|^2 + 1} \right) \frac{\theta_{1,5}\theta_{1,4}}{\theta_{1,2}\theta_{1,3}} \end{aligned}. \tag{13}$$

Outage probability $\mathrm{P}_{out}^{\mathrm{ARQ},1}$ is:

$$\begin{aligned}
&\Pr\left\{SNR_{\mathrm{ARQ},1} < 2^{2R}-1\right\} \\
&= \Pr\left\{\left(\frac{|h_{21}|^2\theta_{1,1}\theta_{1,2}\theta_{1,3}}{\theta_{1,4}\theta_{1,5}} + \frac{\frac{\theta_{1,2}\theta_{1,3}}{{\theta_{1,4}}^2}|h_{R1}|^2|h_{2R}|^2}{\frac{\theta_{1,2}}{\theta_{1,4}}|h_{R1}|^2 + \frac{\theta_{1,3}}{\theta_{1,4}}|h_{2R}|^2 + 1}\right) < \left(2^{2R}-1\right)\frac{\theta_{1,2}\theta_{1,3}}{\theta_{1,4}\theta_{1,5}}\right\} \\
&\approx \frac{1}{2\frac{\sigma_{21}^2\theta_{1,1}\theta_{1,2}\theta_{1,3}}{\theta_{1,4}\theta_{1,5}}} * \left(\frac{\frac{\theta_{1,2}}{\theta_{1,4}}\sigma_{R1}^2 + \frac{\theta_{1,3}}{\theta_{1,4}}\sigma_{R2}^2}{\frac{\theta_{1,2}}{\theta_{1,4}}\sigma_{R1}^2 * \frac{\theta_{1,3}}{\theta_{1,4}}\sigma_{R2}^2}\right)\left(\left(2^{2R}-1\right)\frac{\theta_{1,2}\theta_{1,3}}{\theta_{1,4}\theta_{1,5}}\right)^2 \\
&= \frac{1}{2\sigma_{21}^2\theta_{1,1}\theta_{1,5}} * \left(\frac{\theta_{1,2}\sigma_{R1}^2 + \theta_{1,3}\sigma_{R2}^2}{\sigma_{R1}^2 * \sigma_{R2}^2}\right)\left(\left(2^{2R}-1\right)\right)^2
\end{aligned} \tag{14}$$

After combining the received signals of two time slots, the outage probability of terminal T_1 is as follows:

$$\begin{aligned}
&P_{out}^{\mathrm{t},1} \\
&= 1 - \left(1 - P_{out}^{21} + P_{out}^{21} * \Pr\left(\left(SNR_{\mathrm{ARQ},1} \geq 2^{2R}-1\right) \mid \left(SNR_{21} < 2^{2R}-1\right)\right)\right) \\
&= 1 - \left(1 - P_{out}^{21} + P_{out}^{21} * \frac{\Pr\left(SNR_{21} < 2^{2R}-1\right) - \Pr\left(SNR_{\mathrm{ARQ},1} < 2^{2R}-1, SNR_{21} < 2^{2R}-1\right)}{\Pr\left(SNR_{21} < 2^{2R}-1\right)}\right). \\
&= 1 - \left(1 - P_{out}^{21} + P_{out}^{21} * \left(1 - \frac{P_{out}^{\mathrm{ARQ},1}}{P_{out}^{21}}\right)\right) \\
&= P_{out}^{\mathrm{ARQ},1}
\end{aligned} \tag{15}$$

The outage probability of T_1 received signal is the same as that the traditional HARQ scheme. Similarly, we may get the outage probability $P_{out}^{\mathrm{t},2}$ of T_2 signal (The expression is omitted).

The unification throughput of terminals T_1 and T_2 is $TP_1 = 1 - P_{out}^{\mathrm{t},1}$, $TP_2 = 1 - P_{out}^{\mathrm{t},2}$. The total unification throughput of the system is:

$$TP^T = \frac{TP_1 + TP_2}{2}. \tag{16}$$

The second slot, if T_1 is in SWIPT state, the energy that can be harvested is as follows:

$$E_1^S = (1-\tau)\,\eta\sigma_{R1}^2 P_R. \tag{17}$$

Therefore, the total energy harvested by T_1 is

$$E_1^T = P_{out}^{21} E_1^S + \left(1 - P_{out}^{21}\right) E_1^P. \tag{18}$$

By introducing $P_{out}^{21} = \frac{1}{\sigma_{21}^2}\frac{2^{2R}-1}{\theta_{1,1}}$ into the above formula, the following conclusions can be obtained:

$$
\begin{aligned}
E_1^T &= \frac{1}{\sigma_{21}^2}\frac{2^{2R}-1}{\theta_{1,1}}E_1^S + \left(1-\frac{1}{\sigma_{21}^2}\frac{2^{2R}-1}{\theta_{1,1}}\right)E_1^P \\
&= \eta\sigma_{R1}^2 P_R + \frac{1}{\sigma_{21}^2}\frac{2^{2R}-1}{\theta_{1,1}}\left((1-\tau)\,\eta\sigma_{R1}^2 P_R - \eta\sigma_{R1}^2 P_R\right). \\
&= \eta\sigma_{R1}^2 P_R\left(1-\frac{1}{\sigma_{21}^2}\frac{2^{2R}-1}{\theta_{1,1}}\tau\right)
\end{aligned} \tag{19}
$$

Similarly, the power of the energy harvested by terminal T_2 is easy to be obtained (The expression is omitted).

To sum up, the total average power of energy harvested by the system is:

$$
E^{\mathrm{T}} = \frac{E_1^{\mathrm{T}} + E_2^{\mathrm{T}}}{2}. \tag{20}
$$

In order to describe the performance of the proposed HARQ scheme more comprehensively, the sum function $\Re$ of system throughput and energy acquisition power is constructed:

$$
\Re = TP^{\mathrm{T}} + E^{\mathrm{T}} = \frac{P_{out}^{\mathrm{ARQ},1} + P_{out}^{\mathrm{ARQ},2}}{2} + \frac{\eta\sigma_{R1}^2 P_R\left(1-\frac{1}{\sigma_{21}^2}\frac{2^{2R}-1}{\theta_{1,1}}\tau\right) + \eta\sigma_{R2}^2 P_R\left(1-\frac{1}{\sigma_{12}^2}\frac{2^{2R}-1}{\theta_{2,1}}\tau\right)}{2}. \tag{21}
$$

5 Simulation Analysis

In this section, the correctness of the above analysis is verified by computer simulation. Suppose the variance N_{21}^e, N_{12}^e, N_{R1}^e and N_{R2}^e of signal demodulation noise is 1, the variance of circuit noise is $N_{R1}^c = 0.1$, $N_{R2}^c = 0.1$, energy collection efficiency η is 0.8, the energy ratio of information receiving τ is 0.5, and the information rate threshold R is 1 (*i.e.*, the signal-to-noise ratio satisfies $SNR_{12} < 2^{2*1} - 1$).

The outage probability of full duplex direct link versus power P_2 is presented in Fig. 2. In Fig. 2, the abscissa is the transmitting power P_2 of terminal T_2 in the first time slot, and the ordinate is the outage probability of the signal transmitted by terminal T_2 in the first slot. The parameters are set as follows: the total power of the system is $P_T = 20$ dBW, $P_1 = 0.1\ P$, $P_R = P_T - P_1 - P_2$, the gain of transmission channel is $\sigma_{12}^2 = 1$, $\sigma_{r1}^2 = 1$ and $\sigma_{r2}^2 = 1$, the variance of self-interference is $\sigma_{22}^2 = 0.1$. "Δ" is the Outage probability curve calculated theoretically and "+" is the simulation curve. It is obvious that the theoretical curve coincides with the simulation curve.

For better insights, the throughput of terminal T_2 against power P_2 is given in Fig. 3. In Fig. 3, the abscissa is the transmitting power P_2 of terminal T_2 in the first time slot, the ordinate is the total throughput of terminal T_2 in the two time slots. "Δ" is the throughput curve calculated theoretically. The parameters are the same as those in Fig. 2. When P_2 is small, the throughput of terminal T_2 increases with the increase of P_2. This is because the transmission power of the first slot determines the outage probability of the direct link as shown in Fig. 2. However, when P_2 increases to a certain extent, the transmission power of the relay is severely limited due to the limitation of the total power, which leads to a decrease in the total throughput. Therefore, reasonable power allocation may improve the performance of total throughput.

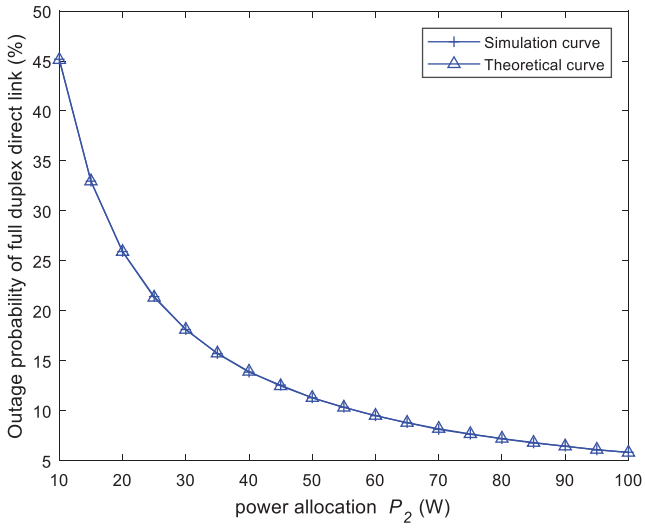

Figure 2: The outage probability of full duplex direct link *vs*. power P_2

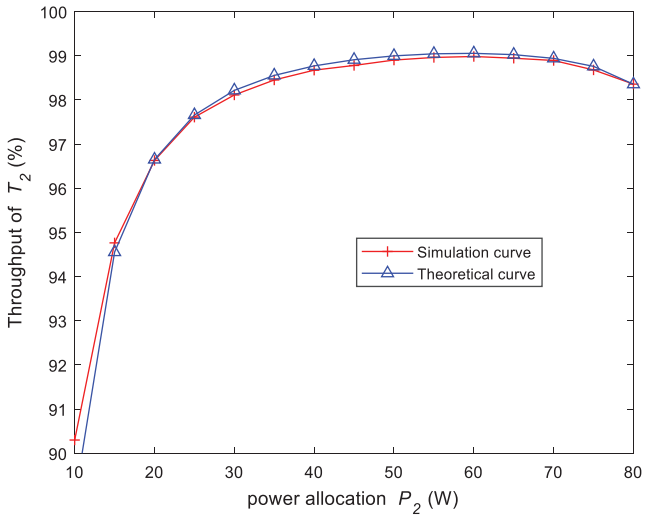

Figure 3: The throughput of terminal T_2 against power P_2

As shown in Fig. 4, the abscissa is the transmission power P_1, and the ordinate is the total throughput of terminal T_2 in two time slots. The total system power is $P_T = 30$ dBW, $P_2 = 0.1\ P$, $P_R = P_T - P_1 - P_2$. Other parameters are the same as those set in Fig. 2. With the increase of P_1, the power used to transmit data of T_2 decreases, especially the forwarding power at the relay. Obviously, the total throughput of terminal T_2 gradually decreases with the increase of P_1.

The relationship between the total throughput of the system and power of the terminal T_2 under the symmetrical channel is indicated in Fig. 5. The parameters in Fig. 5 are the same as those set in Fig. 4, except for $P_T = 30$ dBW, $P_R = 0.1\ P$ and $P_1 = P_T - P_R - P_2$. Because the total throughput of the system is the sum of the throughput of two terminals, little transmission power of terminal T_1 and terminal T_2 may affect the total throughput. As shown in Fig. 5, the total throughput of the system is a symmetric curve. The channel between the two terminals and the relay in Fig. 5 is symmetrical

channel, so the total system throughput reaches the maximum when the two terminals power equals to each other.

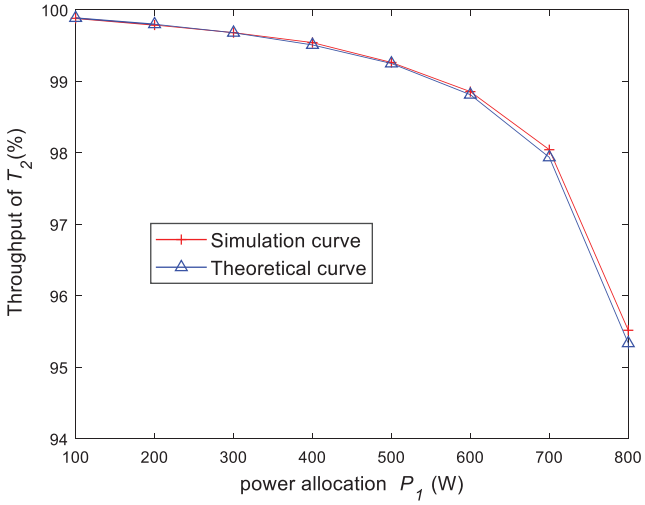

Figure 4: The throughput of terminal T_2 against power P_1

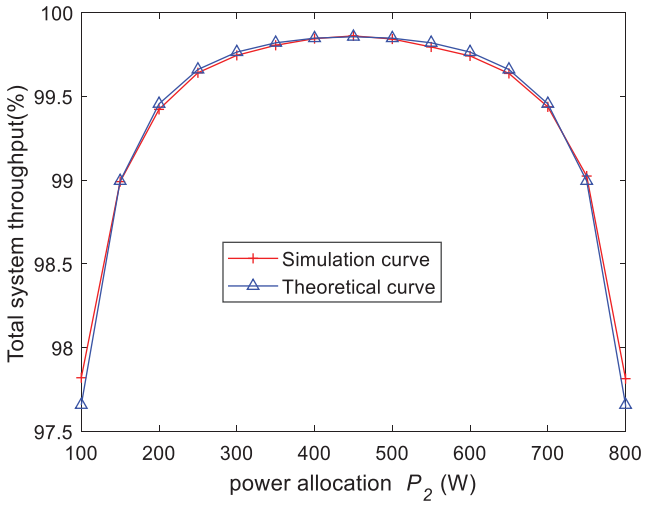

Figure 5: The relationship between the total throughput of the system and power of the terminal T_2 under the symmetrical channel

The total system throughput against P_2 is illustrated in Fig. 6 under asymmetric channel. The parameter is $\sigma_{r1}^2 = 4$ in Fig. 6. In this case, the channel quality from R to terminal T_1 is better than that from R to terminal T_2. In order to achieve the same throughput of two terminals, it is necessary to allocate more power to terminal T_2. As shown in Fig. 6, when the total throughput of the system reaches maximum, the power allocated to terminal T_2 (400 W) is close to and less than the average allocation (450 W).

Fig. 7 compares the energy harvested-throughput sum function of the two schemes in asymmetric channels (the proposed HARQ scheme and the traditional HARQ scheme). Except for $P_T = 25$ dBW,

other parameters are the same as those in Fig. 6. It is obvious that the sum function of the proposed HARQ scheme is better than that of the traditional HARQ scheme. When $P_2 = 22$ dB, the maximum sum function is 54.86% (the proposed HARQ scheme) and 52.307% (the traditional HARQ scheme), respectively.

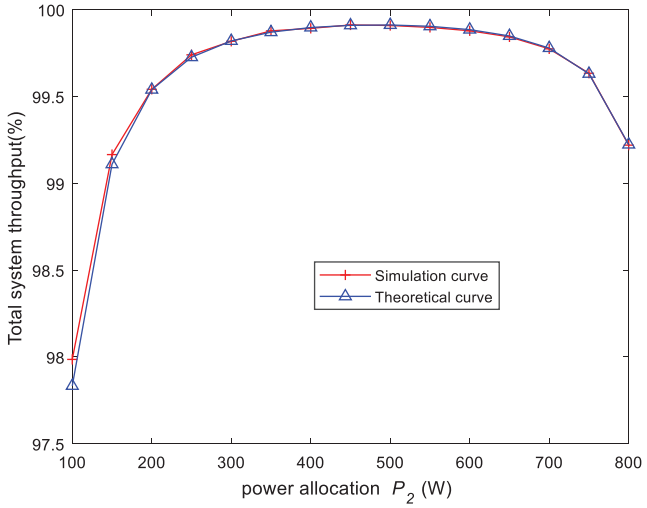

Figure 6: The total system throughput against P_2 under the asymmetric channel

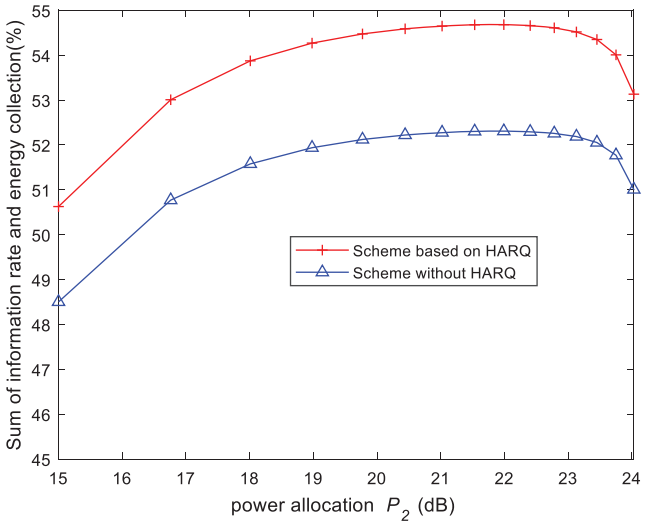

Figure 7: The energy harvested-throughput sum function of the two schemes in asymmetric channels

6 Conclusions

In order to further explore the potential of the SWIPT relay system, the full duplex two-way SWIPT relay HARQ scheme is proposed in this paper. Firstly, the received signal-to-noise ratio (SNR) is calculated by analyzing the system model and time slot structure. Then the outage probability and throughput are obtained by approximate simplification. Then, the energy harvested power in various states is obtained. Finally, the energy harvested-throughput sum function are constructed. Simulation

results show that the proposed HARQ scheme has better energy harvested-throughput sum function than the traditional HARQ scheme.

Acknowledgement: The authors would like to thank the anonymous reviewers for their constructive comments and suggestions.

Funding Statement: This work was supported by the National Natural Science Foundation of China (Grants No. 61701251, 62071244, 62071249, 61872423, 61801236 and 61806100), Open Fund of Key Laboratory of Icing and Anti/De-icing (Grant No. IADL20190105) and the Natural Science Foundation of Jiangsu Province (Grants No. BK20160903).

Conflicts of Interest: The authors declare that they have no conflicts of interest to report regarding the present study.

References

[1] Al-Baidhani, M. Vehkapera and M. Benaissa, "Simultaneous wireless information and power transfer based on generalized triangular decomposition," *IEEE Transactions on Green Communications and Networking*, vol. 3, no. 3, pp. 751–764, 2019.

[2] T. A. Le, Q. Vien, H. X. Nguyen, D. W. K. Ng and R. Schober, "Robust chance-constrained optimization for power-efficient and secure SWIPT systems," *IEEE Transactions on Green Communications and Networking*, vol. 1, no. 3, pp. 333–346, 2017.

[3] Y. Ji, W. Duan, M. Wen, P. Padidar and P. Ho, "Spectral efficiency enhanced cooperative device-to-device systems with NOMA," *IEEE Transactions on Intelligent Transposition Systems*, vol. 99, pp. 1–11, 2020.

[4] H. Zhu, D. Gao and S. Zhang, "A perceptron algorithm for forest fire prediction based on wireless sensor networks," *Journal of Internet of Things*, vol. 1, no. 1, pp. 25–31, 2019.

[5] M. Okhovvat and M. R. Kangavari, "Tslbs: A time-sensitive and load balanced scheduling approach to wireless sensor actor networks," *Computer Systems Science and Engineering*, vol. 34, no. 1, pp. 13–21, 2019.

[6] S. Kaur and V. K. Joshi, "Hybrid soft computing technique based trust evaluation protocol for wireless sensor networks," *Intelligent Automation & Soft Computing*, vol. 26, no. 2, pp. 217–226, 2020.

[7] M. K. Shukla, H. H. Nguyen and O. J. Pandey, "Multiuser full-duplex IoT networks with wireless-powered relaying: Performance analysis and energy efficiency optimization," *IEEE Transactions on Green Communications and Networking*, vol. 4, no. 4, pp. 982–997, 2020.

[8] Y. Yan and S. Zhang, "Energy efficiency maximization of the SWIPT-based full-duplex relay cooperative system," in *Proc. IEEE Int. Conf. on Communication Technology*, Xi'an, China, pp. 398–403, 2019.

[9] X. Shi, J. Sun, D. Li, F. Ding and Z. Zhang, "Rate-energy tradeoff for wireless simultaneous information and power transfer in full-duplex and half-duplex systems," *Computer, Materials and Continua*, vol. 65, no. 2, pp. 1373–1384, 2020.

[10] X. Pei, W. Duan, M. Wen, Y. Wu and V. Monteiro, "Socially-aware joint resource allocation and computation offloading in NOMA-aided energy harvesting massive IoT," *IEEE Internet of Things Journal*, vol. 8, no. 7, pp. 5240–5249, 2021.

[11] K. Xu, Y. Gao, Y. Xu and W. Yang, "Diversity-multiplexing tradeoff analysis of AF two-way relaying channel with hybrid ARQ over rayleigh fading channels," *IEEE Transactions on Vehicular Technology*, vol. 63, no. 3, pp. 1504–1510, 2014.

[12] S. Nam, M. Alouini and S. Choi, "Iterative relay scheduling with hybrid ARQ under multiple user equipment (type II) relay environments," *IEEE Access*, vol. 6, pp. 6455–6463, 2018.

[13] J. Su, R. Xu, S. Yu, B. Wang and J. Wang, "Redundant rule detection for software-defined networking," *KSII Transactions on Internet and Information Systems*, vol. 14, no. 6, pp. 2735–2751, 2020.

[14] D. Kim, S. Park, H. Ju and D. Hong, "Transmission capacity of full-duplex-based two-way ad hoc networks with ARQ protocol," *IEEE Transactions on Vehicular Technology*, vol. 63, no. 7, pp. 3167–3183, 2014.

[15] H. Zhu, B. Smida and D. J. Love, "An efficient network-coded ARQ scheme for two-way wireless communication with full-duplex relaying," *IEEE Access*, vol. 7, pp. 131995–132009, 2019.
[16] V. Towhidlou and M. Shikh-Bahaei, "Improved cognitive networking through full duplex cooperative ARQ and HARQ," *IEEE Wireless Communications Letters*, vol. 7, no. 2, pp. 218–221, 2018.
[17] M. Li, J. Lin, L. Zhong, M. Wang and W. Lv, "Cooperative relay based on exploiting hybrid ARQ," *China Communications*, vol. 16, no. 9, pp. 187–200, 2019.
[18] M. Salehi Heydar Abad, O. Ercetin, T. Elbatt and M. Nafie, "SWIPT using hybrid ARQ over time varying channels," *IEEE Transactions on Green Communications and Networking*, vol. 2, no. 4, pp. 1087–1100, 2018.